Cytotoxic Bisindole Alkaloids from a Marine Sponge *Spongosorites* sp.

Baoquan Bao,[†,‡] Qishi Sun,[‡] Xinsheng Yao,[‡] Jongki Hong,[§] Chong-O. Lee,[⊥] Chung Ja Sim,[∥] Kwang Sik Im,[†] and Jee H. Jung*[,†]

College of Pharmacy, Pusan National University, Busan 609-735, Korea, Shenyang Pharmaceutical University, Shenyang 110-016, People's Republic of China, Korea Basic Science Institute, Seoul 136-701, Korea, Korea Research Institute of Chemical Technology, Daejon 305-343, Korea, and Department of Biology, Hannam University, Daejon 306-791, Korea

Received December 30, 2004

Three new bisindole alkaloids of the hamacanthin class (**1**−**3**) and one new bisindole alkaloid of the topsentin class (**6**) were isolated along with known bisindole alkaloids (**4**, **5**, **7**−**11**) from the MeOH extract of a marine sponge *Spongosorites* sp. by bioactivity-guided fractionation. The planar structures were established on the basis of NMR, MS, and IR spectroscopic analyses. Configurations of compounds **1**−**4** were derived from ^{1}H NMR data and optical rotation. Compounds **1**, **4**, **5**, and **11** showed moderate to significant cytotoxicity against five human tumor cell lines, and compounds **1**−**5** showed weak antibacterial activity against clinically isolated methicillin-resistant strains.

Bisindole alkaloids are recognized as one of the rapidly growing groups of sponge metabolites. The examples reported from marine sponges include topsentins,[1,2] which have a ketone and an imidazole moiety as a linker between two indole rings; nortopsentins,[3] which lack the central ketone observed in topsentins; and dragmacidins[4,5] and hamacanthins,[6,7] which have a piperazine, piperazinone, or pyrazinone moiety as a linker between two indole rings. Some of these metabolites exhibit potent and diverse bioactivities such as cytotoxic,[3,8,9] antitumor,[4] antiviral,[4] antifungal,[3,6] and anti-inflammatory activities.[10] Bisindole alkaloids, such as bromotopsentin, topsentin, nortopsentins A−C, and dragmacidin, were also reported to inhibit the ligand binding to α_{1a} and α_{1b} adrenergic receptors.[11] The α_1 adrenergic antagonists may be considered as potential candidates for treatment of hypertension and benign prostatic hyperplasia.

In our search for bioactive metabolites, three new (**1**−**3**) bisindole alkaloids of the hamacanthin class and a new (**6**) bisindole alkaloid of the topsentin class were isolated by bioactivity-guided fractionation from a marine sponge *Spongosorites* sp. (order Halichondrida, family Halichondriidae) collected off the coast of Jeju Island, Korea. Herein we describe the structure elucidation and the evaluation of cytotoxicity and antibacterial activity of these compounds.

Results and Discussion

(*R*)-6″-Debromohamacanthin A (**1**) was isolated as a yellow amorphous powder. In the FABMS of **1**, the $[M + H]^+$ ion cluster was observed at *m/z* 407/409 in the ratio of 1:1 that is characteristic of a monobrominated compound. The molecular formula was established as $C_{20}H_{15}ON_4Br$ on the basis of the HRFABMS data. The exact mass of the $[M + H]^+$ ions at *m/z* 407.0471 and 409.0530 matched well with the expected molecular formula of $C_{20}H_{16}ON_4{}^{79}Br$ (Δ −3.6 mmu) and $C_{20}H_{16}ON_4{}^{81}Br$ (Δ +4.1 mmu), respectively. The NMR spectra of **1** showed the presence of two indole residues, which were reminiscent of those of hamacanthin A (**12**).[6] The main difference from hamacanthin A was lack of a bromine atom and, accordingly, the presence of an unsubstituted indol-3-yl residue. The 3,6-disubstituted-5,6-dihydro-1*H*-pyrazin-2-one moiety was deduced by a conjugated amide carbonyl carbon (δ_C 157.3, C-2, IR ν_{max} 1693 cm^{-1} due to amide carbonyl), a tetrasubstituted olefinic carbon (δ_C 156.7, C-3), a nitrogen-bearing methine carbon (δ_C 45.8, C-6), and another nitrogen-bearing methylene carbon (δ_C 48.1, C-5) (Table 2). The chemical shift of the carbonyl carbon (δ_C 157.3, C-2) is inconsistent with a ketone functionality as observed in topsentin (**7**) but would fit that of an amide as observed in hamacanthin A (**12**). In the COSY spectrum, the NH proton observed at δ_H 9.76 (H-1) revealed coupling to the methine proton observed at δ_H 5.34 (H-6), which in turn was coupled to the geminal methylene proton signals at δ_H 4.16 (H-5) and 4.25 (H-5). Analysis of ^{1}H, ^{13}C, COSY, and HSQC data, along with comparison of chemical shift values with those of known bisindole alkaloids (**11**),[8] allowed us to establish a 6-bromoindol-3-yl residue and an unsubstituted indol-3-yl residue as partial structures of **1**. Two singlets at δ_H 13.20 (H-1′) and 8.99 (H-2′) and the ABX spin system comprised of signals at δ_H 8.12 (H-4′, d, J = 8.5 Hz), 7.55 (H-5′, dd, J = 8.5, 1.5 Hz), and 7.85 (H-7′, d, J = 1.5 Hz) indicated the presence of a 3,6-disubstituted or 3,5-disubstituted indole moiety (Table 1). The HMBC correlation between the C-3′ (δ_C 106.7) carbon signal and the large doublet proton signal (H-4′, δ_H 8.12, d, J = 8.5 Hz), rather than the small doublet proton signal (H-7′, δ_H 7.85, d, J = 1.5 Hz), along with comparison of chemical shift values with those of known bisindole alkaloids (**8** and **10**),[1,2,8] corroborated the 3,6-disubstitution of the indole moiety. The proton signals at δ_H 11.18 (H-1″), 7.403 (H-2″), 7.76 (H-4″), 7.07 (H-5″), 7.14 (H-6″), and 7.404 (H-7″) indicated the presence of an unsubstituted indole-3-yl moiety. Long-range correlations from H-1″ (δ_H 11.18), H-2″ (δ_H 7.403), H-5 (δ_H 4.25, 4.16), and H-6 (δ_H 5. 34) to C-3″ (δ_C 113.2) and COSY correlation between H-1 (δ_H 9.76) and H-6 (δ_H 5.34) established the connectivity between the dihydropyrazinone ring and the unsubstituted indol-3-yl residue. Although the long-range correlation between the dihydropyrazinone ring and the 6-bromoindol-3-yl moieties was not detected, the connectivity between them was presumed on comparison of chemical shift values with those of hamacanthin A (**12**) (Tables 1 and 2). Therefore, compound **1** was defined as a 6″-

* To whom correspondence should be addressed. Tel: 82-51-510-2803. Fax: 82-51-513-6754. E-mail: jhjung@pusan.ac.kr.
[†] Pusan National University.
[‡] Shenyang Pharmaceutical University.
[§] Korea Basic Science Institute.
[⊥] Korea Research Institute of Chemical Technology.
[∥] Hannam University.

10.1021/np049577a CCC: $30.25
Published on Web 04/26/2005

Table 1. ^{1}H NMR Data of Compounds **1**−**3**, **12**, and **13**[a]

position	1	2	3	12	13
1	9.76 (br s)	9.84 (br s)	11.16 (s)	8.78 (d, 1.0)	8.49 (t, 1.5)
5	4.25 (dd, 15.0, 7.5)	4.23 (dd, 15.0, 7.5)	5.86 (dd, 11.0, 10.0)	4.05 (dd, 16.2, 5.1)	5.25 (dd, 9.5, 4.8)
	4.16 (dd, 15.0, 4.5)	4.16 (dd, 15.0, 4.5)		4.10 (dd, 16.2, 8.5)	
6	5. 34 (dd, 7.5, 4.5)	5.35 (dd, 7.5, 4.5)	4.51 (t, 12.0, 11.0)	4.98 (ddd, 8.5, 5.1, 1.0)	3.61 (ddd, 12.9, 4.8, 1.5)
			4.10 (dd, 12.0, 10.0)		3.47 (ddd, 12.9, 9.5, 1.0)
1′	13. 20 (br s)[b]	13. 20 (br s)[b]	12.96 (br s)	11.59 (d, 2.7)	11.62 (s)
2′	8.99 (s)	9.07 (s)	8.60 (s)	8.41 (d, 2.7)	8.41 (s)
4′	8.12 (d, 8.5)	8.17 (dd, 6.5, 3.0)	8.11 (d, 8.5)	8.29 (d, 8.5)	8.30 (d, 8.7)
5′	7.55 (dd, 8.5, 1.5)	7.41 (m)	7.51 (dd, 8.5, 2.0)	7.20 (dd, 8.5, 2.0)	7.17 (dd, 8.7, 1.6)
6′		7.41 (m)			
7′	7.85 (d, 1.5)	7.67 (dd, 6.5, 3.0)	7.84 (d, 2.0)	7.62 (d, 2.0)	7.63 (d, 1.6)
1″	11.18 (br s)	11.33 (br s)	11.35 (br s)	11.15 (d, 2.3)	11.12 (s)
2″	7.403 (s)	7.45 (s)	7.62 (s)	7.30 (d, 2.3)	7.28 (s)
4″	7.76 (d, 7.5)	7.76 (d, 8.0)	7.58 (d, 7.5)	7.66 (d, 8.5)	7.65 (d, 8.6)
5″	7.07 (t, 7.5)	7.22 (dd, 8.0, 2.0)	7.10 (t, 7.5)	7.13 (dd, 8.5, 2.0)	7.13 (dd, 8.6, 1.6)
6″	7.14 (t, 7.5)		7.18 (t, 7.5)		
7″	7.404 (d, 7.5)	7.60 (d, 2.0)	7.47 (d, 7.5)	7.56 (d, 2.0)	7.59 (d, 1.6)

[a] NMR data of **1**−**3** were measured at 500 MHz in DMSO-d_6 + TFA (ca 1%), while those of **12** and **13** were reported in DMSO-d_6.[6] [b] Signal was assigned by HMBC and COSY experiments.

Table 2. ^{13}C NMR Data of Compounds **1**−**3**, **12**, and **13**[a]

position	1	2	3	12	13
2	157.3	156.8	161.4[b]	157.4	157.2
3	156.7	156.8	161.1[b]	157.6	157.0
5	48.1	47.2	54.8	53.4	53.6
6	45.8	45.5	51.1	46.1	43.2
2′	143.1	144.2	140.6	132.6	132.7
3′	106.7	106.3	113.2	111.0	111.0
3a′	124.1	123.8	123.9	125.0	125.0
4′	123.0	121.1	122.7	124.1	124.1
5′	125.9	124.3	126.5	123.2	123.3
6′	117.0	125.1[c]	117.1	114.7	114.8
7′	116.2	114.5	115.9	114.2	114.1
7a′	138.2	137.4[b]	138.0	137.0	136.9
2″	124.1	125.4[d]	124.7[c]	124.5	123.6
3″	113.2	111.2	111.9	113.1	114.8
3a″	125.2	125.2[c]	124.6[c]	124.6	125.0
4″	119.0	120.7	118.1	120.7	120.8
5″	118.8	122.0	119.3	121.5	121.4
6″	121.7	114.5	121.8	114.7	113.9
7″	111.9	114.0	112.1	114.2	114.2
7a″	136.6	137.5[b]	136.8	137.2	137.2

[a] NMR data of **1**−**3** were measured at 75 MHz in DMSO-d_6 + TFA (ca 1%), while those of **12** and **13** were reported[6] in DMSO-d_6 at 90 MHz. [b,c] Assignments with the same superscript in the same column may be interchanged. [d] Signal was assigned by HMBC experiment.

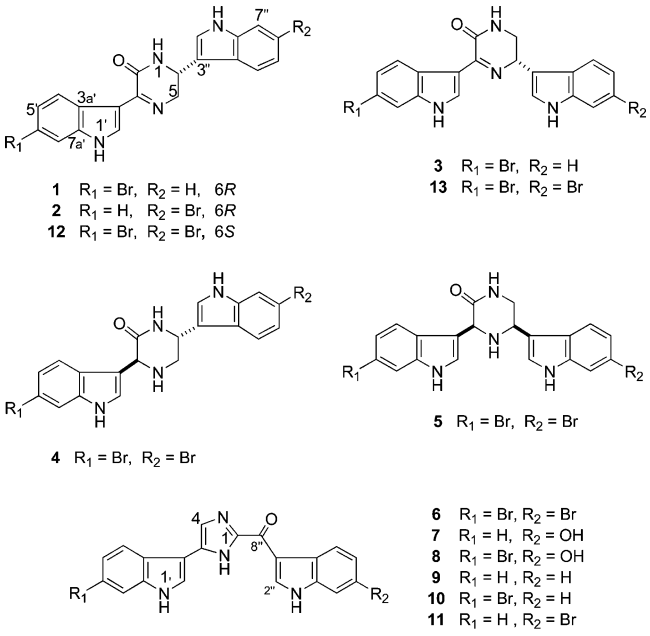

debrominated derivative of hamacanthin A. The absolute configuration of compound **1** was defined on the basis of optical rotation. The optical rotation of **1** (−76°, *c* 0.05, MeOH) was opposite to that of the natural hamacanthin A (+84°, *c* 0.1, MeOH),[6] but was similar to that of the synthetic enantiomer of hamacanthin A, (*R*)-3,6-bis(bromoindol-3-yl)-5,6-dihydro-1*H*-pyrazin-2-one (−79° *c* 0.2, MeOH),[12] indicating that compound **1** has an *R* configuration.

(*R*)-6′-Debromohamacanthin A (**2**) was also isolated as a yellow amorphous powder. Its molecular formula was established as $C_{20}H_{15}ON_4Br$ on the basis of HRFABMS data. In the FABMS, the $[M + H]^+$ ion cluster was observed at *m/z* 407/409 in the ratio of 1:1. The exact mass of the $[M + H]^+$ ions at *m/z* 407.0478 and 409.0524 matched well with the expected molecular formula of $C_{20}H_{16}ON_4{}^{79}Br$ (Δ −2.9 mmu) and $C_{20}H_{16}ON_4{}^{81}Br$ (Δ +3.5 mmu), respectively. The NMR spectra of **2** also showed the presence of two indole residues, which were reminiscent of those of hamacanthin A (**12**),[6] and the compound possesses the indol-3-yl, 6-bromoindol-3-yl, and 3,6-disubstituted-5,6-dihydro-1*H*-pyrazin-2-one moieties. Careful examination of the ^{1}H, COSY, and HMBC data suggested that the bromine atom was located on the indole ring of the right half of compound **2**. The ABX spin system comprised of the signals at δ_H 7.76 (H-4″, d, J = 8.0 Hz), 7.22 (H-5″, dd, J = 8.0, 2.0 Hz), and 7.60 (H-7″, d, J = 2.0 Hz) indicated the presence of a 3,6-disubstituted or 3,5-disubstituted indole moiety. The long-range correlation between signals of H-4″ (δ_H 7.76, d, J = 8.0 Hz) and C-3″ (δ_C 111.2) corroborated the 3,6-disubstitution of the indole moiety. Long-range correlations from H-5 and H-6 to C-3″ (δ_C 111.2) and from H-6 to C-3a″ (δ_C 125.2) established the connectivity between the dihydropyrazinone ring and the 6-bromoindole residue. The connectivity between the dihydropyrazinone ring and the unsubstituted indol-3-yl residue was presumed on comparison of chemical shift values with those of hamacanthin A (**12**) (Tables 1 and 2). Thus, compound **2** was defined as a 6′-debrominated derivative of hamacanthin A. The optical rotation of **2** (−91°, *c* 0.2, MeOH) was opposite that of the natural hamacanthin A (+84°, *c* 0.1, MeOH),[6] but was similar to that of the synthetic enantiomer of hamacanthin A, (*R*)-3,6-bis(bromoindol-3-yl)-5,6-dihydro-1*H*-pyrazin-2-one (−79° *c* 0.2, MeOH),[12] indicating that compound **2** also has an *R* configuration. It is unexpected to observe that the stereochemistry of **1** and **2** are opposite to that of hamacanthin A (**12**). However, the

Table 3. ^{1}H and ^{13}C NMR Data of Compounds **6**, **10**, and **11**[a,b]

	6		**10**		**11**	
	δ_C	δ_H	δ_C	δ_H	δ_C	δ_H
2	143.3		141.7		142.9	
4	114.9	7.96 (s)	116.9	7.96 (s)	118.7	7.91 (s)
5	129.9[c]		131.2		133.1	
1′		11.69 (br s)		11.67 (br s)		11.54 (br s)
2′	125.1[e]	8.08 (br s)	127.0	8.07 (d, 2.5)	124.8	8.06 (d, 2.5)
3′	105.4[c]		103.6		105.0	
3a′	123.2		123.8		124.6	
4′	121.2	8.01 (d, 8.0)	121.6	8.05 (d, 8.5)	119.7	8.02 (d, 8.0)
5′	122.4	7.28 (dd, 8.0, 1.5)	123.9	7.30[d]	120.3	7.21 (td, 8.0, 1.0)
6′	113.6[c]		115.7		122.3	7.16 (dt, 8.0, 1.0)
7′	114.3	7.68 (d, 1.5)	115.5	7.69 (d, 1.5)	112.3	7.48 (d, 8.0)
7a′	137.0		137.9		136.6	
1″		12.46 (br s)		12.38 (br s)		12.43 (br s)
2″	137.9	9.00 (s)	139.1	8.96 (s)	138.6	9.03 (s)
3″	113.3		114.2		113.8	
3a″	124.8[e]		126.3		125.5	
4″	122.8	8.26 (d, 8.5)	121.9	8.33 (dd, 7.0, 2.5)	123.3	8.28 (d, 8.5)
5″	124.9[e]	7.44 (dd, 8.5, 1.5)	123.7	7.30[d]	125.4	7.43 (dd, 8.5, 1.5)
6″	114.3		124.8	7.30[d]	116.2	
7″	115.5	7.78 (d, 1.5)	113.4	7.58 (dd, 8.5, 1.5)	115.5	7.78 (d, 1.5)
7a″	137.0		137.5		137.6	
8″	174.1		172.7		174.1	

[a] ^{13}C NMR data of **6** were obtained in DMSO-d_6 + TFA (ca 1%) at 75 MHz, and the ^{13}C NMR data of **10** and **11** were reported[8] in DMSO-d_6 + TFA (ca 1%) at 125 MHz. [b] ^{1}H NMR data were measured at 500 MHz in DMSO-d_6 + TFA (ca 1%). [c] Signals were assigned by HMBC experiment. [d] Overlapped signals. [e] Assignments with the same superscript in the same column may be interchanged.

stereochemistry of **1** and **2** is consistent with that of *trans*-3,4-dihydrohamacnathin A (**4**).

(*S*)-6″-Debromohamacanthin B (**3**) was also isolated as a yellow amorphous powder. Its molecular formula was established as $C_{20}H_{15}ON_4Br$ on the basis of FABMS data. The exact mass of the $[M + H]^+$ ions at *m/z* 407.0494 and 409.0530 matched well with the expected molecular formula of $C_{20}H_{16}ON_4{}^{79}Br$ (Δ −1.3 mmu) and $C_{20}H_{16}ON_4{}^{81}Br$ (Δ +4.1 mmu), respectively. The NMR data indicated the presence of a 3,6-disubsitituted indole, 3-substituted indole, and 3,5-disubstituted-5,6-dihydro-1*H*-pyrazin-2-one moieties. In the COSY spectrum, H-1 (δ_H 11.16) showed couplings to the geminal methylene protons at δ_H 4.51 (H-6, t, J = 12.0, 11.0 Hz) and 4.10 (H-6, dd, J = 12.0, 10.0 Hz), which in turn were coupled to the methine proton at δ_H 5.86 (H-5, dd, J = 11.0, 10.0 Hz). Long-range C−H correlations were observed from H-1 (NH, δ_H 11.16) to C-2 (δ_C 161.4) and from H-5 (1H, δ_H 5.86) to C-3 (δ_C 161.1). These observations confirmed the presence of the dihydropyrazinone ring system and the substitution of the indole-3-yl group at C-5. Thus, compound **3** was defined as a 6″-debrominated derivative of hamacanthin B (**13**).[6] The specific rotation of compound **3** was +43° (*c* 0.3, MeOH). Comparison with the natural hamacanthin B (+176°)[6] and the synthetic (*S*)-hamacanthin B (+183°)[13] suggested that compound **3** also has the same *S* configuration.

Dibromodeoxytopsentin (**6**) was also isolated as a yellow amorphous solid. Its molecular formula was established as $C_{20}H_{15}ON_4Br_2$ on the basis of the ^{1}H and ^{13}C NMR and FABMS data. In the FABMS of **6**, the $[M + H]^+$ ion cluster was observed at *m/z* 483/485/487 in the ratio of 1:2:1, which is characteristic of a dibrominated compound. The ^{1}H NMR data of **6** were similar to those of reported topsentin derivatives, bromodeoxytopsentin (**10**)[8] and isobromodeoxytopsentin (**11**),[8] indicating the same structural framework. As reported previously for topsentins,[1,2,8] broadening or doubling of ^{1}H NMR signals of compounds **6**−**11** was observed in neutral solutions (CD_3OD, acetone-d_6, or DMSO-d_6) due to slow interconversion of imidazolylmethanone tautomers and/or rotamers. This phenomenon is likely a result of a combination of tautomerism and rotational isomerism of the imidazolylmethanone, as there expected to be a potential hydrogen bonding between the ketone carbonyl and imidazole NH. The ^{1}H NMR signals became uncomplicated in acidic condition due to rapid interconversion. In contrast, the ^{1}H NMR spectra of compounds **1**−**5** showed no such broadening or doubling in neutral solutions (CD_3OD, DMSO-d_6), which is a notable difference between these two classes of compounds.

The clear difference between compound **6** and bromodeoxytopsentin (**10**) was the presence of an additional bromine substitution and, accordingly, the presence of two independent 6-bromoindol-3-yl moieties. The chemical shifts for C-2 (δ_C 143.3), C-4 (δ_C 114.9), C-5 (δ_C 129.9), and H-4 (δ_H 7.96) were in agreement with those reported for topsentins.[3,7,8] Two independent 6-bromoindol-3-yl moieties were delineated on the basis of the proton signals at δ_H 12.46/9.00/8.26/7.78/7.44 and δ_H 11.69/8.08/8.01/7.68/7.28. Furthermore, long-range correlation from C-5 (δ_C 129.9) to H-2′ (δ_H 8.08) established the connectivity between the imidazole ring and the bromoindol-3-yl moiety. Long-range correlation between the imidazole ring and another bromoindol-3-yl moiety was not detected, but the connectivity between them was presumed on comparison of chemical shift values with those of isobromodeoxytopsentin (**11**) (Table 3). Thus, compound **6** was defined as a dibrominated derivative of deoxytopsentin (**9**).[1] A compound with the same structure as **6** was erroneously referred to as isobromotopsentin,[5] although the original structure of isobromotopsentin was published 3 years beforehand.[16] To the best of our knowledge, compound **6** is a new chemical entity.

Seven known bisindole alkaloids (**4**, **5**, and **7**−**11**) were also isolated as yellow amorphous powders. Compounds **4** and **5** possessed dihydrohamacanthin skeletons and were identified as *trans*-3,4-dihydrohamacanthin A and *cis*-3,4-dihydrohamacanthin B,[7] respectively. The relative stereochemistry at positions C-3 and C-6 of the central piperazinone ring of compound **4** was established as *trans* on the basis of the diaxial coupling (J = 11.0 Hz) between the H-6$_{ax}$ (δ_H 5.31) and H-5$_{ax}$ (δ_H 3.71) protons and the dipolar correlation between H-3 (δ_H 5.70) and H-5$_{ax}$ in the ROESY spectrum (Figure 1). The conformer (**B**) with the bulky

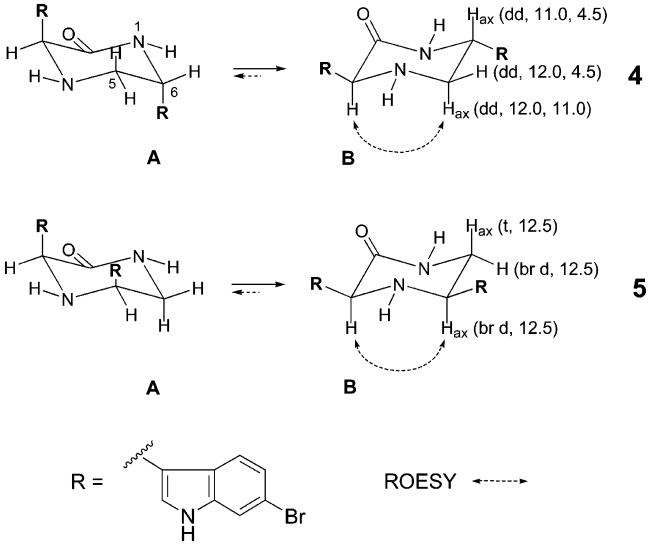

Figure 1. Relative configurations of compounds **4** and **5**.

indole rings at equatorial positions would be predominant, while the contribution of the alternative conformer (**A**) would be negligible. The absolute configuration of compound **4** was determined as (3*S*,6*R*) on the basis of optical rotation. The specific rotation of **4** (+16°, *c* 1.1, MeOH) was similar to that of the natural *trans*-3,4-dihydrohamacanthin A (+5.3°, *c* 0.2, MeOH),[7] but opposite to that of the synthetic enantiomer,[15] (3*R*,6*S*)-3,6-bis(6-bromo-1*H*-indol-3-yl)piperazin-2-one (−6°, *c* 0.275, MeOH/acetone = 1:1).

The relative stereochemistry of compound **5** was defined as *cis* on the basis of the diaxial coupling ($J = 12.5$) between H-5 (δ_H 5.37) and H-6 (δ_H 4.07) and the NOE correlation between H-3 (δ_H 5.71) and H-5 (δ_H 5.37) (Figure 1). The absolute configuration of compound **5** remains to be determined.

Compounds **7**−**11** were identified as topsentin (**7**),[1] bromotopsentin (**8**),[1] deoxytopsentin (**9**),[1] bromodeoxytopsentin (**10**),[8] and isobromodeoxytopsentin (**11**),[8] respectively. It was previously reported that topsentin (**7**) and bromotopsentin (**8**) show cytotoxicity against P388 with IC_{50} values of 2.0 and 7.0 μg/mL, respectively.[3] Bromodeoxytopsentin (**10**) and isobromodeoxytopsentin (**11**) were reported to exhibit cytotoxicity against the human leukemia cell-line K-562 with IC_{50} values of 0.6 and 2.1 μg/mL, respectively.[8] Compounds **1**−**11** were evaluated for cytotoxicity against a panel of five human tumor cell lines. Compounds **1**, **4**, **5**, and **11** showed moderate to significant cytotoxicity to all of the cancer cell lines tested (Table 4). The lipophilicity (estimated on the basis of HPLC retention time) may modulate the in vitro cytotoxicity of compounds **1**−**5**. Of the piperazinone derivatives (**4** and **5**, relative retention times: $t_{R5} > t_{R4}$), the more lipophilic derivative (**5**) showed higher activity. Of the dihydropyrazinone derivatives (**1**−**3**, relative retention times: $t_{R1} > t_{R2} > t_{R3}$), the most lipophilic derivative (**1**) again showed the highest activity. The substitution pattern of piperazinone or dihydropyrazinone ring may not play a crucial role in the modulation of the in vitro cytotoxicity of these compounds, because compound **5** displayed higher activity than **4**, while compound **3** displayed lower activity than **1**.

Compounds **1**−**11** were also evaluated for antibacterial activity against 20 clinically isolated methicillin-resistant strains, and compounds **1**−**5** showed weak antibacterial activity against nine of the 20 strains in different degree (Table 5). It is noteworthy that hamacanthins (**1**−**5**) showed antibacterial activity, while the topsentins (**6**−**11**) did not show any activity at the highest concentration tested (MIC values >25 μg/mL).

Table 4. Cytotoxicity Data of Compounds **1**−**11**[a]

compound	A549	SK-OV-3	SK-MEL-2	XF498	HCT15
1	5.61	4.20	4.73	4.12	3.58
2	>30.0	>30.0	>30.0	>30.0	26.91
3	>30.0	>30.0	>30.0	>30.0	>30.0
4	8.28	8.03	9.14	6.88	5.35
5	3.41	3.62	3.85	3.22	2.83
6	>30.0	>30.0	>30.0	>30.0	>30.0
7	>30.0	>30.0	>30.0	>30.0	13.33
8	>30.0	28.14	7.02	14.99	>30.0
9	>30.0	>30.0	>30.0	>30.0	26.18
10	>30.0	>30.0	>30.0	>30.0	11.48
11	12.30	8.70	4.54	5.51	6.38
doxorubicin	0.01	0.03	0.01	0.01	0.05

[a] Data expressed in ED_{50} values (μg/mL). A549, human lung cancer; SK-OV-3, human ovarian cancer; SK-MEL-2, human skin cancer; XF498, human CNS cancer; HCT 15, human colon cancer.

Experimental Section

General Experimental Procedures. Optical rotations were measured using a JASCO DIP-370 digital polarimeter. CD spectra were recorded using a JASCO J-715 spectropolarimeter (sensitivity 50 mdeg, resolution 0.2 nm). IR spectrum was recorded using a JASCO FT/IR-410 spectrometer. ^1H and ^{13}C NMR spectra were recorded on Bruker AC300 and Varian INOVA 500 instruments. Chemical shifts were reported with reference to the respective residual solvent or deuterated solvent peaks (δ_H 2.5 and δ_C 39.5 for DMSO-d_6). FABMS data were obtained on a JEOL JMS SX-102A. HPLC was performed with a YMC ODS-H80 column (250 × 10 mm, 4 μm, 80 Å) using a Shodex RI-71 detector.

Animal Material. The sponges were collected by hand using scuba (20 m depth) in October 2002, off the coast of Jeju Island, Korea. The collected sample was a loose association of two sponges *Spongosorites* sp. and *Halichondria* sp. The two sponges were separated, and only *Spongosorites* sp. was subjected to chemical analysis. The thin and dark orange outer layer, 5 mm thick, was identified as *Halichondria* sp. It has medium oxea (140−200 × 6−8 μm). The surface of the body was smooth. The texture was easily broken. Oscules, 1−2 mm in diameter, were scattered on the surface. The yellow inner layer, 5 cm thick, was identified as *Spongosorites* sp., the surface of which was completely covered by *Halichondria* sp. This species has small oxea (70−90 × 2 μm), medium oxea (130−260 × 7−9 μm), and large oxea (400−850 × 9−15 μm). The texture was easily broken. A voucher specimen (registry No. Spo. 44) is deposited at the Natural History Museum, Hannam University.

Extraction and Isolation. The frozen sponge (0.8 kg) was chopped into small pieces and extracted with MeOH at room temperature. The MeOH extract showed significant toxicity to brine shrimp larvae (LD_{50} 23.7 μg/mL). The MeOH extract was partitioned between CH_2Cl_2 and water. The CH_2Cl_2 layer was further partitioned between aqueous MeOH and *n*-hexane. The aqueous MeOH fraction was subjected to stepped gradient reversed-phase flash column chromatography (YMC Gel ODS-A, 60 Å, 230 mesh) with a solvent system of 60 to 100% MeOH/H_2O to afford 16 fractions. Fraction 11 (3.45 g), one of the bioactive fractions (LD_{50} 14.7 μg/mL), was subjected to reversed-phase HPLC eluting with 75% MeOH to afford compounds **6** (2.1 mg), **7** (2.4 mg), **10** (3.2 mg), and **11** (5.1 mg) and subfraction 11-1. Compounds **8** (2.3 mg) and **9** (3.7 mg) were obtained by separation of subfraction 11-1 on a reversed-phase HPLC eluting with 63% MeCN. Fraction 2 (800 mg), one of the bioactive fractions (LD_{50} 33.9 μg/mL), was subjected to reversed-phase HPLC (YMC ODS-H80 column) eluting with 75% MeOH to afford compound **4** (11.0 mg) and 13 subfractions. Compound **5** (8.0 mg) was obtained by separation of subfraction 2-11 on a reversed-phase HPLC eluting with 65%

Table 5. Antibacterial Activity Data of Compounds **1**−**5**[a]

compound	A	B	C	D	E	F	G	H	I
1	25.0	>25.0	>25.0	25.0	>25.0	>25.0	>25.0	25.0	>25.0
2	12.5	12.5	25.0	12.5	12.5	12.5	12.5	25.0	12.5
3	25.0	25.0	>25.0	25.0	25.0	25.0	25.0	25.0	25.0
4	12.5	>25.0	>25.0	>25.0	>25.0	>25.0	>25.0	>25.0	>25.0
5	12.5	25.0	>25.0	12.5	25.0	25.0	25.0	25.0	25.0
imipenem	0.004	0.004	0.781	0.013	0.013	0.007	0.195	0.098	0.195
meropenem	0.007	0.007	6.250	0.098	0.195	0.049	0.025	0.098	0.049

[a] Data expressed in MIC values (μg/mL). A, *Streptococcus pyogenes* 308A; B, *Streptococcus pyogenes* 77A; C, *Streptococcus faecium* MD 8b; D, *Streptococcus aureus* SG 511; E, *Streptococcus aureus* 285; F, *Streptococcus aureus* 503; G, *Escherichia coli* DC 2; H, *Pseudomonas aeruginosa* 1771M; I, *Klebsiella oxytoca* 1082 E.

MeCN. Subfraction 2-12 was subjected to successive reversed-phase HPLC eluting with 71% MeOH to afford compounds **2** (2.8 mg), **3** (3.0 mg), and **11** (2.6 mg). Compound **1** (1.5 mg) was obtained by separation of subfraction 2-14 on a reversed-phase HPLC eluting with 73% MeOH.

(***R*)-6″-Debromohamacanthin A (1):** yellow amorphous powder; $[\alpha]^{23}_D$ −76° (*c* 0.05, MeOH); CD (*c* 1 × 10^{-4} M, MeOH) $\Delta\epsilon$ (nm) −6.83 (320), −8.35 (414); IR (film) ν_{max} (cm^{-1}) 1693; ^{1}H NMR data, see Table 1; ^{13}C NMR data, see Table 2; LRFABMS *m/z* 407/409 $[M + H]^+$; FAB-CID MS/MS *m/z* 362/364 $[M + H - COOH]^+$ (0.05); HRFABMS *m/z* 407.0471/409.0530 (calcd for $C_{20}H_{16}ON_4{}^{79}Br$, 407.0507; $C_{20}H_{16}ON_4{}^{81}Br$, 409.0489).

(*R*)-6′-Debromohamacanthin A (2): yellow amorphous powder; $[\alpha]^{23}_D$ −91° (*c* 0.2, MeOH); CD (*c* 1 × 10^{-4} M, MeOH) $\Delta\epsilon$ (nm) − 6.12 (328), − 8.94 (412); IR (film) ν_{max} (cm^{-1}) 1693; ^{1}H NMR data, see Table 1; ^{13}C NMR data, see Table 2; LRFABMS *m/z* 407/409 $[M + H]^+$; HRFABMS *m/z* 407.0478/409.0524 (calcd for $C_{20}H_{16}ON_4{}^{79}Br$, 407.0507; $C_{20}H_{16}ON_4{}^{81}Br$, 409.0489).

(*S*)-6″-Debromohamacanthin B (3): yellow amorphous powder; $[\alpha]^{23}_D$ +43° (*c* 0.3, MeOH); CD (*c* 1 × 10^{-4} M, MeOH) $\Delta\epsilon$ (nm) − 5.40 (338); IR (film) ν_{max} (cm^{-1}) 1693; ^{1}H NMR data, see Table 1; ^{13}C NMR data, see Table 2; LRFABMS *m/z* 407/409 $[M + H]^+$; HRFABMS *m/z* 407.0494/409.0530 (calcd for $C_{20}H_{16}ON_4{}^{79}Br$, 407.0507; $C_{20}H_{16}ON_4{}^{81}Br$, 409.0489).

***trans*-3,4-Dihydrohamacanthin A (4):** pale yellow amorphous powder; $[\alpha]^{21}_D$ +16° (*c* 1.1, MeOH); LRFABMS *m/z* 487/489/491 $[M + H]^+$; HRFABMS *m/z* 486.9752/488.9752/490.9767 (calcd for $C_{20}H_{16}ON_4{}^{79}Br_2$, 486.9769; $C_{20}H_{16}ON_4{}^{79}Br^{81}Br$, 488.9750; $C_{20}H_{16}ON_4{}^{81}Br_2$, 490.9733).

***cis*-3,4-Dihydrohamacanthin B (5):** yellow amorphous powder; $[\alpha]^{21}_D$ +101° (*c* 0.8, MeOH); LRFABMS *m/z* 487/489/491 $[M + H]^+$.

Dibromodeoxytopsentin (6): yellow amorphous powder; ^{1}H and ^{13}C NMR data, see Table 3; LRFABMS *m/z* 483/485/487 $[M + H]^+$.

Topsentin (7): yellow amorphous solid; LRFABMS *m/z* 343 $[M + H]^+$.

Bromotopsentin (8): yellow amorphous powder; LRFABMS *m/z* 421/423 $[M + H]^+$.

Deoxytopsentin (9): yellow amorphous powder; LRFABMS *m/z* 329 $[M + H]^+$.

Bromodeoxytopsentin (10): yellow amorphous powder; LRFABMS *m/z* 405/407 $[M + H]^+$.

Isobromodeoxytopsentin (11): yellow amorphous powder; LRFABMS *m/z* 405/407 $[M + H]^+$.

Evaluation of Cytotoxicity. The rapidly growing cells were harvested, counted, and inoculated at the appropriate concentrations ((1−2) × 10^4 cells/well) into 96-well microtiter plates. After incubation for 24 h, the compounds dissolved in culture medium (RPMI 1640, Gibco; 10% FBS, Gibco) were applied to the culture wells in triplicate followed by incubation for 48 h at 37 °C under a 5% CO_2 atmosphere. The culture was fixed with cold TCA and stained by 0.4% SRB (sulforhodamine B, Sigma) dissolved in 1% acetic acid. After solubilizing the bound dye with 10 mM unbuffered Tris base by a gyrotatory shaker, the absorbance at 520 nm was measured with a microplate reader (Dynatech Model MR 700). Fifty percent inhibitory concentration (ED_{50}) was defined as the concentration that reduced absorbance by 50% compared to the control level in the untreated wells.

Evaluation of Antibacterial Activity. Mueller Hinton agar plates were impregnated with 17 serial dilutions of the sample and standards (meropenem and imipenem) to make a final concentration of 25 to 0.002 μg/mL. The strains were inoculated into Fleisch extract broth (containing 10% horse serum depending on strains) and incubated for 18 h at 37 °C. The cultured strains were inoculated onto the Mueller Hinton agar plates with 104 CFU per spot population by automatic inoculater (Dynatech). The MIC was measured after 18 h of incubation.

Acknowledgment. The study was supported by a grant from the Korea Research Foundation (2003-041-E 00331).

Supporting Information Available: ^{1}H NMR data of compounds **7**−**9**, ^{13}C NMR and ^{1}H data of compounds **4** and **5**. This material is available free of charge via the Internet at http://pubs.acs.org.

References and Notes

(1) Bartic, K.; Braekman, J. C.; Daloze, D.; Stoller, C.; Huysecom, J.; Vandevyver, G.; Ottinger, R. *Can. J. Chem.* **1987**, *65*, 2118−2121.
(2) Tsujii, S.; Rinehart, K. L. *J. Org. Chem.* **1988**, *53*, 5446−5453.
(3) Sakemi, S.; Sun, H. H. *J. Org. Chem.* **1991**, *56*, 4304−4307.
(4) Wright, A. E.; Pomponi, S. A.; Cross, S. S.; McCarthy, P. *J. Org. Chem.* **1992**, *57*, 4772−4775.
(5) Capon, R. J.; Rooney, F.; Murray, L. M.; Collins, E.; Sim, A. T. R.; Rostas, J. A. P.; Butler, M. S.; Carroll, A. R. *J. Nat. Prod.* **1998**, *61*, 660−662.
(6) Gunasekera, S. P.; McCarthy, P. J.; Kelly-Borges, M. J. *J. Nat. Prod.* **1994**, *57*, 1437−1441.
(7) Casapullo, A.; Bifulco, G.; Bruno, I.; Riccio, R. *J. Nat. Prod.* **2000**, *63*, 447−451.
(8) Shin, J.; Seo, Y.; Cho, K. W.; Rho, J. R.; Sim, C. J. *J. Nat. Prod.* **1999**, *62*, 647−649.
(9) Morris, S. A.; Andersen, R. J. *Tetrahedron* **1990**, *46*, 715−720.
(10) Jacobs, R. S.; Pomponi, S.; Gunasekera, S.; Wright, A. *PCT Int. Appl.* **1998**, 45.
(11) Phife, D. W.; Ramos, R. A.; Feng, M.; King, I.; Gunasekera, S. P.; Wright, A.; Eatel, M.; Patchier, J. A.; Coval, S. J. *Bioorg. Med. Chem. Lett.* **1996**, *6*, 2103−2106.
(12) Jiang, B.; Yang, C. G.; Wang, J. *J. Org. Chem.* **2001**, *66*, 4865−4869.
(13) Jiang, B.; Yang, C. G.; Wang, J. *J. Org. Chem.* **2002**, *67*, 1396−1398.
(14) Murray, L. M.; Lim, T. K.; Hooper, N. A.; Capon, R. J. *Aust. J. Chem.* **1995**, *48*, 2053−2058.
(15) Yang, C. G.; Wang, J.; Tang, X. X.; Jiang, B. *Tetrahedron: Asymmetry* **2002**, *13*, 383−394.
(16) Murray, M. L.; Lim, K. T.; Hooper, J. N. A.; Capon, R. J. *Aust. J. Chem.* **1995**, *48*, 2053−2058.

NP049577A